JOURNAL OF APPLIED ELECTROCHEMISTRY 23 (1993) 957–965

Characterization of anodically formed polypyrrole/tungsten trioxide composites

M. DAHLHAUS, F. BECK

Fachgebiet Elektrochemie, University of Duisburg, Lotharstrasse 1, D-4100 Duisburg 1, Germany

Received 21 July 1992; revised 12 January 1993

Composite PPy/WO_3 materials were synthesized anodically under various conditions. The cyclovoltammetric switching curves are very close to the blank polypyrrole. The redox behaviour of the filler is only detected through electrochromism, leading to a yellow grey colour at +0.4 V vs SCE and to a green surface at −0.6 V. For overoxidation of the composite, a degree of overoxidation $Y = 5$ is found, the same as for the matrix alone. Photoelectrochemical response is due to the conducting polymer at negative potentials and even at 0 V vs SCE. A strong effect at positive potentials is due to the WO_3 pigment. From this, a flat band potential of +0.15 V vs SCE is determined for aqueous 0.1 M $LiClO_4$. Some non-electrochemical properties are also reported. Surface roughness increases with increasing WO_3 concentration, but for thicker layers, from MeCN, it decreases. SEM micrographs reveal homogeneous distribution of WO_3. Large secondary particles are observed in NBu_4BF_4 electrolyte. True and nominal thicknesses differ by up to a factor 1.65 due to the porous structure and this explains differences between densities measured by the flotation and the jump method. X-ray diffraction analysis exhibits unchanged WO_3-lines, but no PPy-lines due to the amorphous character. The conductivity of the composite from MeCN is much lower than expected by the volume filling of the WO_3.

1. Introduction

Polymers with an intrinsic electronic conductivity are new materials, which have attracted much interest. A convenient method for their preparation is based on the film forming anodic polymerization of suitable monomers, which are predominantly 5-ring heterocycles. One of the most important is pyrrole. Electrodeposition of polypyrrole (PPy) may be effected from aqueous [1, 2] as well as from non-aqueous [3, 4] electrolytes. A very broad variation of the polymer properties is possible by modification of the monomer structure, mainly via N-substitution, via the nature of the doping anion [5] and through composites with a conventional polymer matrix [6].

It is only recently that the opposite case of a composite material was realized. The polypyrrole made up the continuous matrix, and highly dispersed materials were incorporated by electrophoresis [7–9] or in strongly agitated electrolytes [10–12]. The latter method parallels the cathodic formation of metal composites, known for four decades [13, 14]. In a previous paper [12], the codeposition of polypyrrole and tungsten trioxide powder was described. It is the aim of the present report to characterize the properties of this novel composite material.

2. Experimental details

Conditions for the galvanostatic codeposition of the PPy/WO_3 composites have already been described in [12]. Only a short summary is needed here. The two electrolytes each contained 0.1 M $LiClO_4$ in

(I) MeCN, 0.1 M H_2O, $j = 0.5\,mA\,cm^{-2}$, and
(II) H_2O, $j = 2\,mA\,cm^{-2}$.

From 0.01 up to 30 g dm^{-3} WO_3 was dispersed in the electrolyte. Four modes of convection were employed, a rotating (sheet) electrode (RE), pumping in a loop (PL), ultrasonic stirring (US) and a cell with an intensive stirrer (IS). Depending on the mode of characterization, two kinds of materials were used: (a) coated cylindrical Pt-electrode, $A = 0.5\,cm^2$, 1 mm diameter, for all electrochemical measurements; $d_n = 1–10\,\mu m$; and (b) free standing foils, $d_n = 10\,\mu m$, peeled off from a polished stainless steel sheet electrode, each side $A = 15\,cm^2$.

The potentiodynamic switching curves of the blank and the WO_3-loaded PPy-layers were obtained at voltage scan rates of 2 and 20 mV s^{-1} in the monomer-free, nonstirred base electrolytes. A conventional set up of a potentiostat, voltage scan generator and electronic data acquisition system in combination with a HP 7090 A measurement plotting system was employed.

The photoelectrochemical response was investigated in various electrolytes under illumination of a 1 cm^2 Pt-electrode, coated with the PPy/WO_3-layer, $d_n = 1$ to $3\,\mu m$, with the light of a high pressure Hg-lamp (Osram, HBO, 100 W), focussed to about 1 cm^2 area. The energy was provided by a PRA M 303 power supply. The

light was chopped with a frequency of about $0.07\,s^{-1}$.

The electrical resistivity of free standing films was measured with the aid of a four point probe (Alessi, CPS-06). Determination of surface roughness of the coatings was done with a mechanical profilometer (Perth-o-meter, Feinprüf GmbH, Göttingen), using various tracing systems, *cf.* [15]. Tensile strength was determined with a home made machine, using a variety of spring balances up to 10 N.

All potentials quoted in this work refer to the NaCl saturated calomel electrode (SSCE). This reference electrode is +236 mV vs SHE. The measurements were performed at 20 °C under nitrogen in slowly stirred electrolytes.

3. Results and discussion

3.1. Electrochemical behaviour

3.1.1. Potentiodynamic switching curves: The possibility of anodic doping/undoping of polypyrrole is well known from the initial work of Diaz *et al.* [16]. Anions are inserted/released for charge compensation, but cations may also participate (*cf.* [17] and the literature cited therein). The question arises, whether the redox behaviour of the matrix is changed through the presence of the WO_3 filler, and if WO_3 itself shows any redox activity. The experiments were performed in the monomer-free electrolytes, as already mentioned in Section 2. The composites from the aqueous electrolyte II were characterized in the aqueous base electrolyte and *vice versa.*

The standard nominal thickness d_n of the polypyrrole coating was 10 μm. The maximum voltage scan rate, v_S, which is compatible with this d_n can be calculated:

$$v_S = \frac{\Delta U D}{d^2} \qquad (1)$$

where $\Delta U = 2\,V$ is the voltage range and $D = 10^{-10}\,cm^2\,s^{-1}$ is the diffusion coefficient in the PPy matrix. This leads to $0.2\,mV\,s^{-1}$. However, as the composite is a porous material (see below), higher scan rates of $2\,mV\,s^{-1}$ are allowable. Even at $20\,mV\,s^{-1}$, no distinct loss of redox capacity was detected.

The slow cyclovoltammetric profile for electrolyte II (H_2O) is shown in Fig. 1. No large differences between the blank polypyrrole and the composite can be seen, either in the first discharge curve or in the steady state cyclic curves. The charge under the first discharge curve clearly exceeds that under the steady state curves. A slight depolarization is obtained for PPy/WO_3 in the positive (charging) direction. Similar effects were found previously for PPy/TiO_2 [12]. These findings are attributed to an enhanced porous structure in the presence of the filler, leading to a decrease in local current densities.

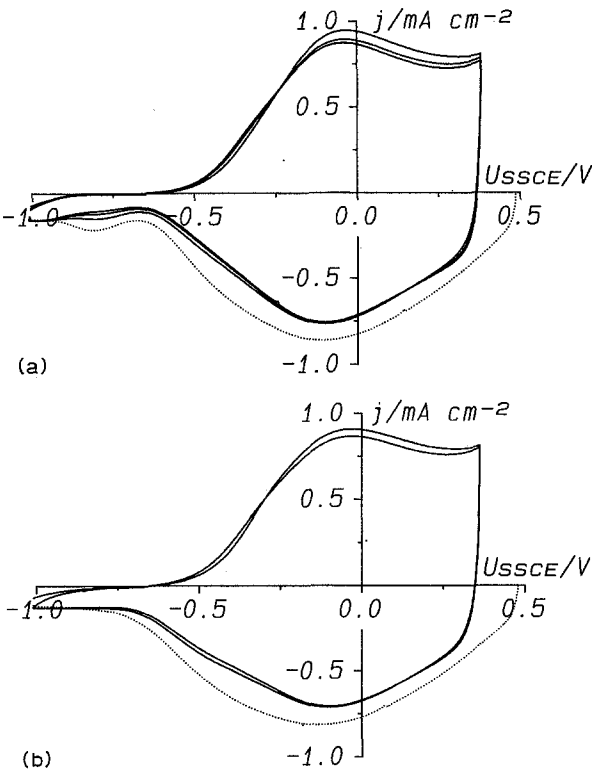

Fig. 1. Cyclovoltammetric response of blank and WO_3 filled PPy-electrodes, $d_n = 10\,\mu m$, $v_S = 2\,mV\,s^{-1}$. The PPy-layers were anodically deposited from aqueous electrolyte II and cycled in 0.1 M $LiClO_4$ in H_2O (a) Blank PPy: (·····) first discharge; (——) three following cycles. (b) WO_3 filled PPy, 20 wt % WO_3: (·····) first discharge; (——) two following cycles.

If the nonaqueous electrolyte I (MeCN) is used (Fig. 2), the anodic depolarization for filled PPy is somewhat larger. Current peaks for first discharge and periodic recharge are sharper and occur at

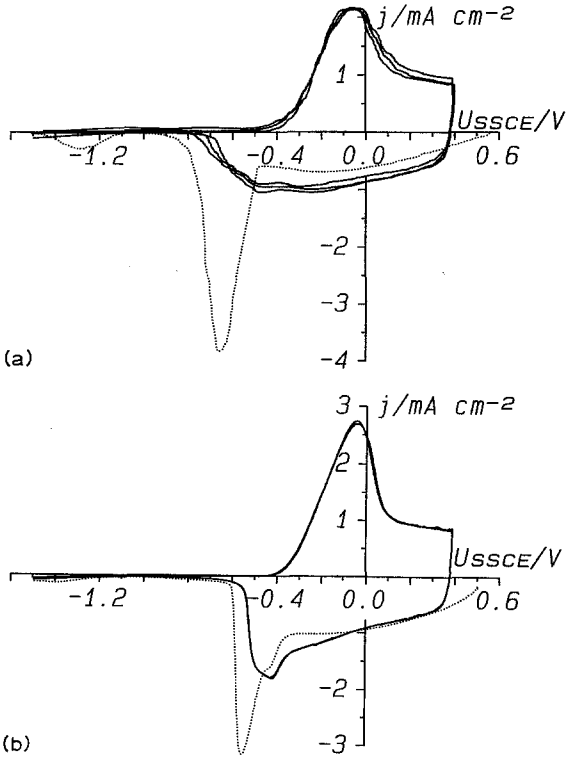

Fig. 2. The same as for Fig. 1 but with electrolyte I (MeCN). Cycling in 0.1 M $LiClO_4$ in MeCN. (a) Blank PPy; (b) WO_3 filled PPy, 25 wt % WO_3.

lower overvoltages. The current efficiencies for the potentiodynamic cycling,

$$\gamma = \frac{Q_-}{Q_+} \tag{2}$$

where Q_+ is the anodic charge capacity and Q_- the cathodic discharge capacity, were found to be virtually quantitative.

The degrees of insertion y (defined as the molar redox capacity per mole of monomer), can be calculated from the charge for the electrodeposition Q_o and the first discharge capacity ($Q_{E,0}$) as follows, where γ is the current efficiency:

$$y_1 = \frac{2Q_{E,o}}{\gamma(Q_o - Q_{E,o})} \tag{3}$$

It is also possible to use the steady state discharge capacity (Q_E), which leads then to another y:

$$y_2 = \frac{2Q_E}{\gamma(Q_o - Q_E)} \tag{4}$$

Table 1 compiles the y values for three thicknesses and two electrolytes.

y_1 is appreciably higher than y_2. This is probably due to the fact that a reduction of acid ($HClO_4$), which is stored in the pores, occurs in the course of the first discharge

$$HClO_4 + e^- \rightarrow \tfrac{1}{2}H_2 + ClO_4^-, \tag{5}$$

but not in the steady state. On average, $y = 33\%$ for MeCN and $y = 25\%$ for H_2O. The presence of WO_3 in the composite has only a minor influence on y, which is somewhat higher than in the blank polypyrrole.

Interestingly, the intrinsic redox properties of WO_3 itself are not seen in the composite. The thermodynamic potential for $WO_3 \rightarrow W_2O_5$ is -0.5 V and the reaction should be detectable. This may be due to at least two factors:

(i) a lack of proton activity. Nonaqueous systems inhibit the redox activity, e.g. for NiO_x [18].

Table 1. Reversible redox capacity of PPy and PPy/WO_3
Cyclic voltammetry at 2 mV s^{-1}. The current density for electrodeposition was 0.5 mA cm^{-2} for entries 3–8, 2 mA cm^{-2} for entry 9 and 10, but 0.05 mA cm^{-2} for entry 1 and 2

No.	$d_n/\mu m$	c_C wt %(WO_3)	y_1	y_2
I(MeCN)				
1	1	–	0.67	0.37
2	1	10	0.51	0.39
3	3	–	0.32	
4	10	–	0.37	0.30
5	10	10	0.43	0.31
II(H_2O)				
6	1	–	0.37	0.24
7	3	–	0.27	0.28
8	3	30	–	0.30
9	10	–	0.20	0.15
10	10	10	0.21	0.16

(ii) transport limitation of water and/or acid in the strictly hydrophobic polymer matrix.

As a consequence, a cycling experiment was undertaken in 0.1 M $HClO_4$ (instead of $LiClO_4$) in water. However, even under these conditions, no additional reduction step was observed.

On the other hand, a pronounced electrochromic behaviour was noted. The freshly prepared composite electrode has a yellow–grey colour, the WO_3 itself is yellow. In the course of the first discharge in electrolyte I (MeCN), this turns to grey at 0.3 V, to brown-green at -0.1 V and to an intensive green at the sharp peak at -0.6 V. On reoxidation, the initial colour, yellow–grey, is restored reversibly after charging up to 0.4 V. Electrochromism could only be observed at electrodes from electrolyte I, measured in 0.1 M $LiClO_4$ in acetonitrile. It was even enhanced in case of bromide electrocatalysis during electrodeposition [12]. However, no electrochromism was found if 0.1 M $LiClO_4$ in *water* was employed as electrolyte for the measurements.

This electrochromism does not contradict the lack of additional redox capacity, for only the surface of the WO_3-particles at the surface of the composite must be reduced. The ratio of the redox capacities in a PPy: $WO_3 = 1:1$ composite is about 1:0.1. Moreover, the WO_3 reduction proceeds only to 3% to yield tungsten bronzes, which have an intensive blue colour [19, 20]:

$$WO_3 + xH^+ + xe^- \rightarrow WO_3H_x \tag{6}$$

Regarding the limitations mentioned above, the ratio can easily attain extreme values such as 1:0.03 or less.

3.1.2. Anodic overoxidation. The anodic overoxidation of polypyrrole is an irreversible process, which proceeds at potentials positive to the reversible doping/undoping reaction [21–23]. The degree of overoxidation is defined as

$$Y = \frac{Q_{oo}}{Q_{E,o}} \tag{7}$$

where Q_{oo} is the charge under the overoxidation peak and $Q_{E,o}$ is the reversible redox capacity. Y depends on the nucleophile. If it is water, $Y = 5$ is found, which is interpreted in terms of the anodic formation of 4-hydroxy-pyrollinone(3) units at every third ring, with the radical cation as an intermediate. The conjugation is interrupted.

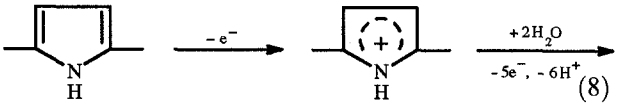

(8)

Figure 3 shows the potentiodynamic overoxidation of blank polypyrrole and of PPy/WO_3 composites in electrolyte II (H_2O). The reversible switching peaks are well separated from the large overoxidation peaks. The following degrees of overoxidation Y

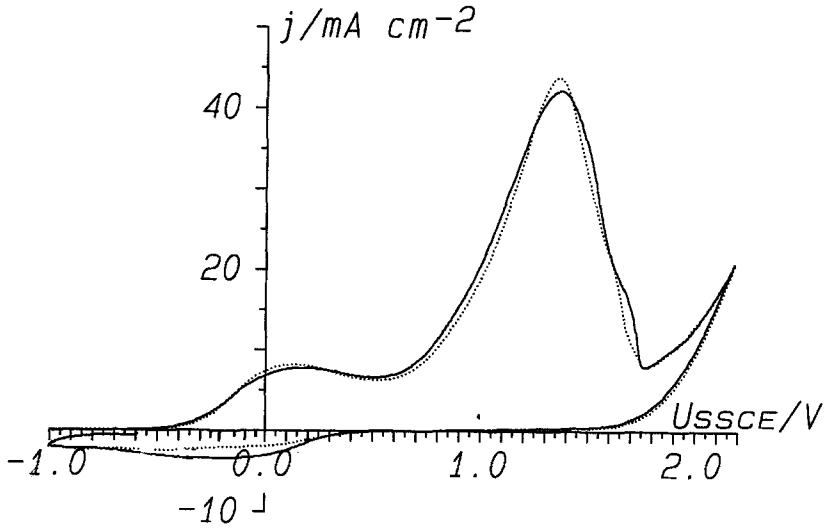

Fig. 3. Anodic overoxidation of blank polypyrrole (·····) and of polypyrrole with 20 wt % WO_3 (——) in 0.1 M $LiClO_4(H_2O)$. $d_n = 10\,\mu m$, $v_S = 20\,mV\,s^{-1}$. The potentiodynamic curves were measured after three reversible cycles (−1 ... 0.4 V) at $2\,mV\,s^{-1}$.

were found, with the values for the blank polypyrrole in parantheses:

Electrolyte I: $Y = 3.2$ (3.2)

Electrolyte II: $Y = 5.1$ (5.7)

No strong effects were found in the presence of WO_3. This shows, that the electroorganic oxidation in the solid state is only a matter of reactivity of the polymer backbone and the availability of the nucleophiles in the solid. Catalytic effects due to the interfaces PPy/WO_3 are not detectable.

3.1.3. Photoelectrochemical response: Both components in the PPy/WO_3 composite are known to exhibit a photoelectrochemical response, depending on the potential. The *polypyrrole* matrix was formerly believed to show a photoeffect only in the undoped state due to the transition of the metal behaviour to that of a p-semiconductor at negative potentials [24]. However, later a distinct photocurrent was detected in the partially doped state at 0 V vs SCE [25]. This finding was confirmed for polyaniline [26–28] and for polycarbazole [29]. We have measured a pronounced photocurrent at positive potentials, *cf.* Fig. 4. The effect increases at more positive potentials. It is also influenced by the voltage scan rate; the time for the light and dark periods were constant at 10 s.

Two measurements at improved time resolutions are shown in the following two Figures. Polypyrrole layers 3 μm thick were electrodeposited onto the cylindrical stainless steel cover of a thermoelement. The photocurrent and the temperatures could be measured simultaneously. These measurements were performed at constant potentials, after reaching a quasisteady state of the dark current near zero in the course of about 5 min. Figure 5 displays an example in 0.1 M $LiClO_4$ in H_2O at 0 V vs SSCE. The photocurrent rises steeply, while the temperature increases slowly in the course of the whole light period. In the dark, the photocurrent decays rapidly, while the temperature falls slowly. Clearly a relatively fast photoelectrochemical response is observed in the doped state. The slow process may be a temperature response, eventually superimposed by a

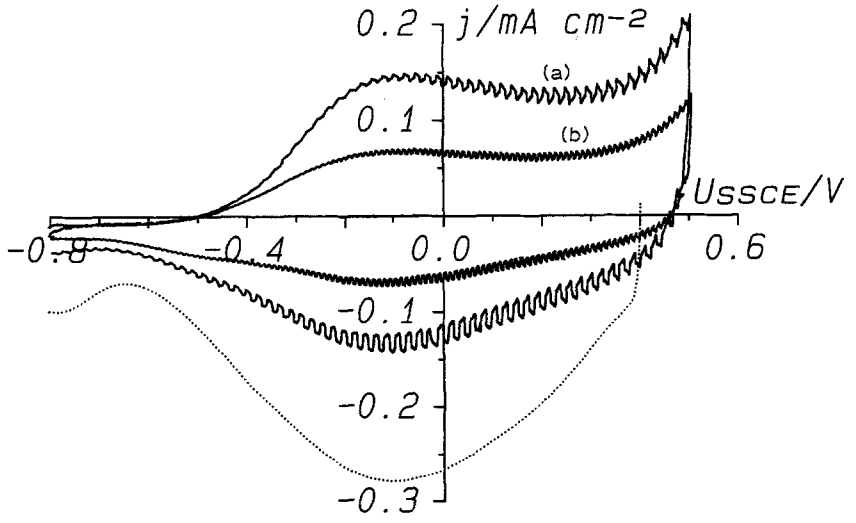

Fig. 4. Photoelectrochemical response of a blank PPy-layer, $d_n = 3\,\mu m$, in 0.1 M $LiClO_4(H_2O)$. The PPy was electrodeposited from aqueous electrolyte II. Light/dark periods each 10 s. (·····) First discharge: $2\,mV\,s^{-1}$. (a) 1st cycle: $1\,mV\,s^{-1}$ and (b) 2nd cycle: $0.5\,mV\,s^{-1}$.

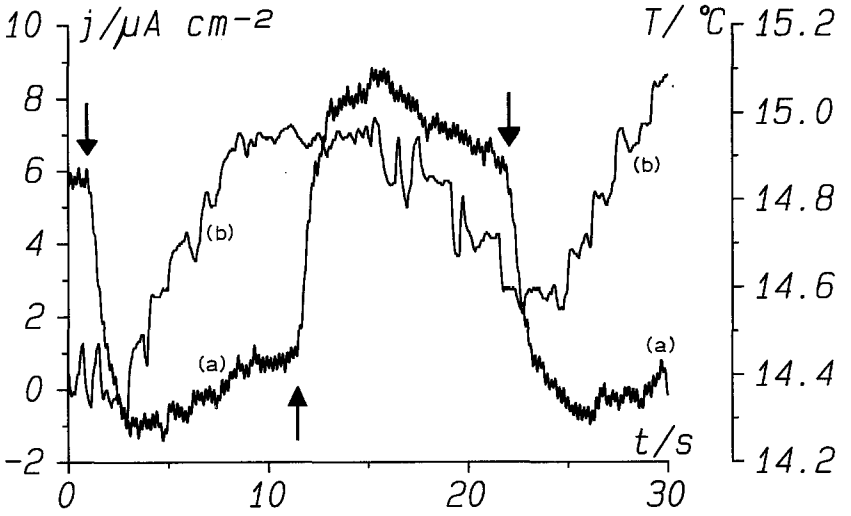

Fig. 5. Photoelectrochemical response of a blank PPy-layer at $U_{SSCE} = 0\,V$, $d_n = 3\,\mu m$ (see text). The layer was electrodeposited from electroloyte II (H_2O) and measured in 0.1 M $LiClO_4$ (H_2O). (a) Current density against time. (b) Electrolyte temperature against time. Positive scan direction: (↓) light on; (↑) light off.

slow photoeffect. By contrast, only a slow response could be detected in this potential region for the non-aqueous electrolyte, 0.1 M $LiClO_4$ in acetonitrile, in parallel with the heating/cooling cycle. However, at negative potentials in the undoped state, strong and rapid photoelectrochemical responses were found, as shown in Fig. 6. These negative potentials were not established in the aqueous electrolytes due to a strong increase in the rate of hydrogen evolution.

The other component in the new composite is WO_3. Again, this filler displays a photoelectrochemical response by itself, as found previously for TiO_2 in PPy/TiO_2 [7, 11]. WO_3 and TiO_2 are n-type semiconductors, and photoelectrochemical response can be expected at positive potentials. This is also found for the PPy/WO_3 composite, as shown in Fig. 7. The effect, starting at 0.15 V and increasing continuously at more positive potentials, clearly exceeds the response, which is due to the PPy matrix, and which can be seen at more negative potentials. According to Fig. 8, the photocurrent pulses were plotted vs. the potential. Extrapolation to zero photocurrent led to a flat band potential [30] of +0.15 V vs SSCE. This is in good agreement with data reported in the literature from measurements at thermally grown WO_3 layers on tungsten [30–34], at anodically prepared oxide-layers on the metal [33, 35–37], at W-oxide layers obtained through thermal decomposition of ammonium tungstate [31] or of metal–organic precursors [38] sputtering of WO_3 [32], vacuum evaporation of WO_3 [35], vapour transport [39] or at $PTFE/WO_3$ pressed powder composites [40]. The band gap is reported to be 3.2 eV, sometimes the values are down to 2.4 eV. The present results demonstrate, that the WO_3/PPy composite electrode exhibits a typical WO_3-photoresponse. The intrinsic photoeffect for the PPy matrix itself is much weaker, if present at all, and it does not interfere negatively with the WO_3 response. It should be noted that these measurements are only of a qualitative character, for no correlation with the absorption of the material was performed. An

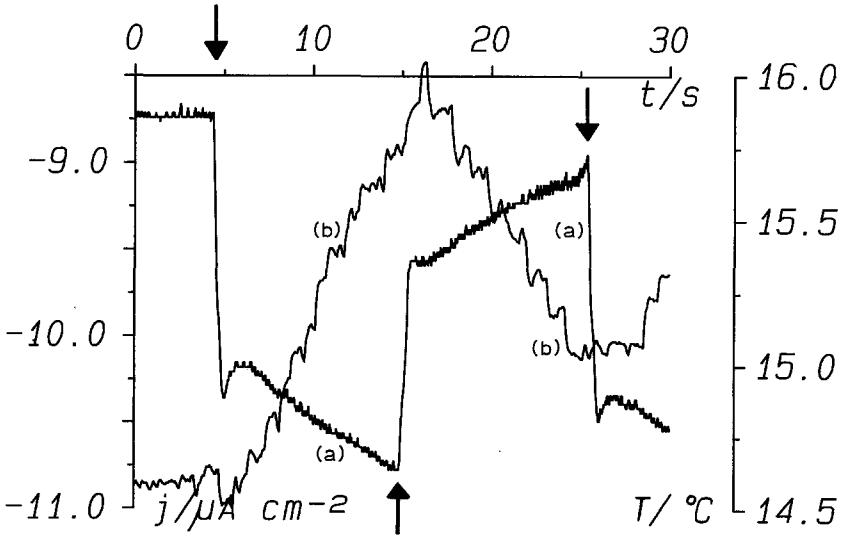

Fig. 6. Photoelectrochemical response at $U_{SSCE} = -1.3\,V$ of a blank PPy-layer, $d_n = 3\,\mu m$, see text. The layer was electrodeposited from electrolyte I (MeCN) and measured in 0.1 M $LiClO_4$ in MeCN. (a) Current density against time. (b) Electrolyte temperature against time. Negative scan direction: (↓) light on; (↑) light off.

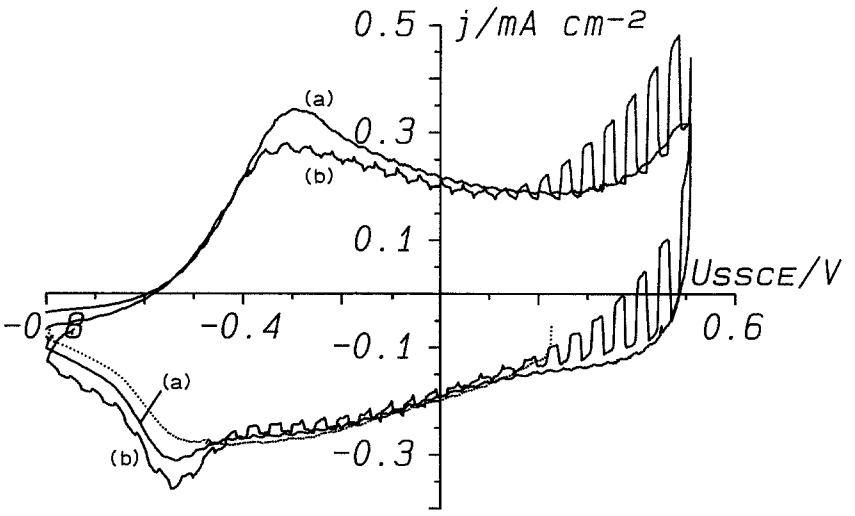

Fig. 7. Potentiodynamic current voltage curves of a PPy-layer ($d_n = 2\,\mu m$), from electrolyte I, MeCN, with 25 wt % WO_3. The measurement was performed in 0.1 M $LiClO_4$ in H_2O. (·····) First discharge. (a) Basic curve in the dark, and (b) illumination with chopped light.

improved yield could be expected with a transparent matrix. However, polypyrrole must then be substituted by polythiophene (derivatives) due to the instability of PPy in the reduced (transparent) state. The polythiophenes are stable against air in the undoped state. A possible problem may arise due to the enhanced photoeffect of the matrix in the semiconducting state. These systems are under investigation.

3.2. *Nonelectrochemical properties*

3.2.1. Surface properties: Surface roughness was measured with a profilometer. The average roughness R_a was obtained by averaging all roughness elongations. Figure 9 shows R_a in dependency on c_C. In electrolyte I (MeCN), R_a is relatively high, and increases with increasing c_C. The tendency is the same for the composite from electrolyte II for the thinner layer, $d_n = 3\,\mu m$. The layers are much smoother. Surprisingly, the thicker layer ($d_n = 10\,\mu m$) shows the opposite tendency. The layer becomes smoother with increased WO_3-loading. A possible explanation may be that hydrogen bubbles adhere strongly at the unfilled or weakly filled PPy films, but not at all at the highly filled ones. As expected, R_a increases with d_n. Another value R_z can be derived from these measurements. R_z is the average roughness depth. For an exact definition *cf.* [15]. In general, $R_z > R_a$, and the influence of c_C and d_n is qualitatively the same. As an example R_z decreases in the last mentioned example from $29\,\mu m$ at $c_C = 0$ to $13\,\mu m$ at $c_C = 35$ wt %.

SEM micrographs for three thicknesses at a constant WO_3-concentration, $c_C = 10\,g\,WO_3\,dm^{-3}$, are displayed in Fig. 10. An invariant surface density of the pigment is observed at different c_C, as formerly with TiO_2 [12], and this supports the previous conclusion that the bulk distribution of the pigment is uniform [12]. The particle size is in the region 5–10 μm, in agreement with direct measurements reported in [12]. Submicron particles can be recognized, however. Surprisingly, the WO_3 particles adhere to the 'summits' of the PPy-matrix rather than in the 'valleys'.

Figure 11 exhibits a microphotograph for a PPy/WO_3 composite deposited from an electrolyte containing 0.1 M NBu_4BF_4 and 1 mM NBu_4Br (catalyst) in acetonitrile; this is called electrolyte III. Much larger secondary particles with a diameter of about 60 μm are incorporated due to agglomeration.

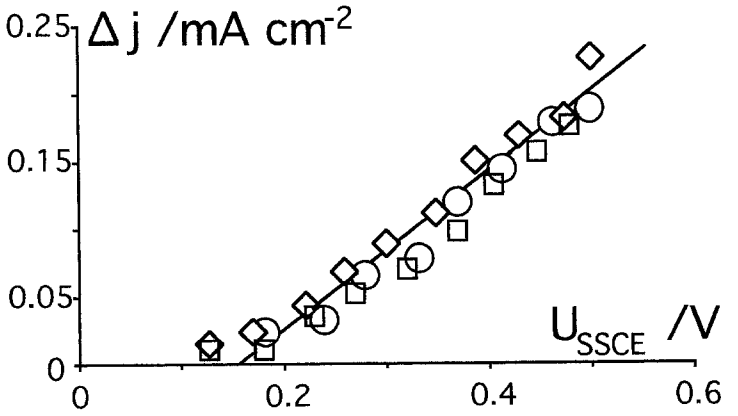

Fig. 8. A plot of photocurrent amplitudes versus the potential. (◇) Forward scan, $d_n = 3\,\mu m$, (□) back scan, $d_n = 3\,\mu m$, and (○) forward scan, $d_n = 2\,\mu m$.

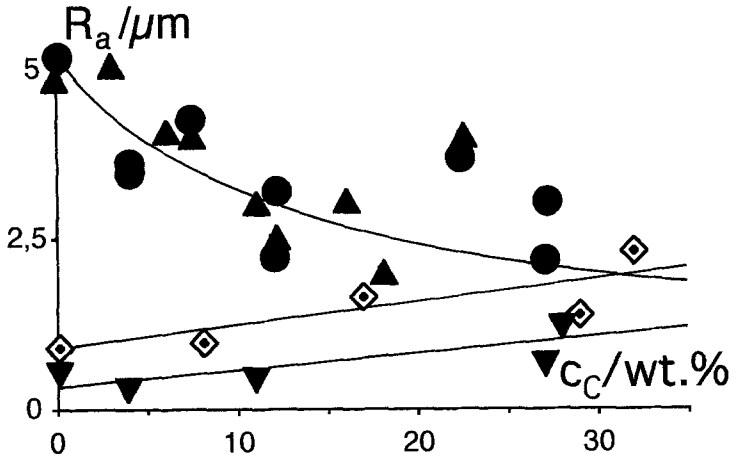

Fig. 9. Average roughness of WO_3 filled PPy-layers in dependency on the WO_3 concentrations in the composite. (◇) From electrolyte I (MeCN), $d_n = 3\,\mu m$, (▼) from electrolyte II (H_2O), $d_n = 3\,\mu m$, and (▲●) from electrolyte II (H_2O), $d_n = 10\,\mu m$.

This may occur under the influence of the quaternary ammonium-ions NBu_4^+, which act as surfactants. Similar effects have been found in the composite PPy/TiO_2 under these conditions [11]. No effect was found for the $LiClO_4$-electrolyte.

3.2.2. Bulk Properties: The true thickness, d, of the composite polymer layers was measured with the profilometer, using the so called jump method [15]. These d values are compiled in Table 2, in conjunction with the nominal thickness d_n, which is characteristic for the compact material [41]. The contribution of the filler was neglected in this case, for it does not exceed 10% even at 30 wt % loading. It is found, that $d > d_n$ (with one exception), which is due to the porosity of the material.

Table 2 also contains several densities ρ. The theoretical density ρ_{th} was calculated from the concentration c_C and the densities of the compact materials, $\rho = 1.50$ for PPy from electrolyte I (MeCN), $\rho = 1.55$ for PPy from electrolyte II (H_2O) and $\rho = 7.16$ for WO_3. The first two values were measured by the flotation method. The first value compares well with $\rho = 1.48$, measured through the same method by Diaz *et al.* [42]. The other flotation densities ρ_F are also shown in Table 2, and are close to ρ_{th}, indicating a quantitative penetration of the porous material by the mixed organic solvent. A third density, ρ_J, was derived from the true thickness d, found through the jump method, as mentioned above:

$$\rho_J = \rho_{th}(d_n/d) \tag{9}$$

These densities are much lower than ρ_F, due to the porosity P [43]. P can be calculated according to

$$P = 1 - (d_n/d) = 1 - (\rho_J/\rho_F) \tag{10}$$

and the porosity data are shown in the last column of Table 2. P is higher for electrolyte I than II, and it increases with the thickness of the composite layer.

X-ray diffraction analysis discloses the typical lines for WO_3. No change with respect to the free pigment

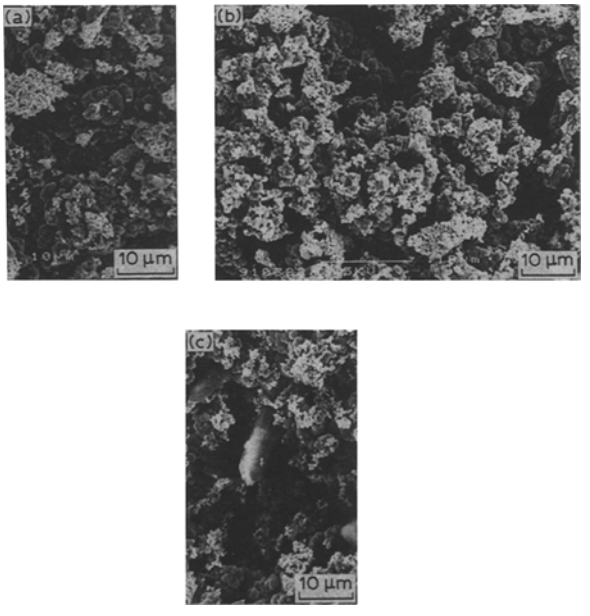

Fig. 10. SEM micrographs for PPy/WO_3-composites, electrodeposited from aqueous electrolyte II (PL). The concentrations of the WO_3 in the electrolyte was 10 g dm^{-3}, corresponding to 20 wt % in the composite. The nominal thicknesses are (a) $d_n = 3\,\mu m$, (b) $d_n = 10\,\mu m$ and (c) $d_n = 30\,\mu m$.

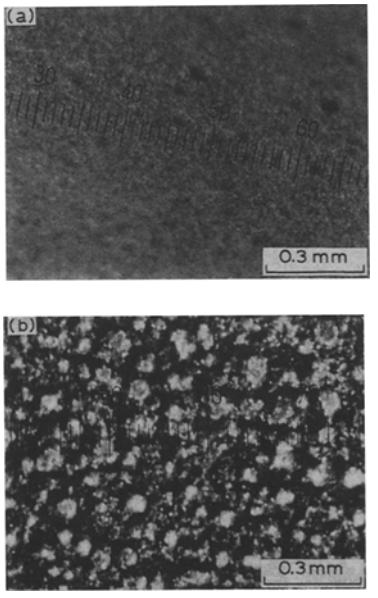

Fig. 11. Light microscopic micrographs of PPy/WO_3 composites from electrolyte I (MeCN), $d_n = 10\,\mu m$. The concentrations of WO_3 in the electrolyte were: (a) 10 g dm^{-3}, 0.1 M $LiClO_4$, PL, and (b) 20 g dm^{-3}, 0.1 M $NBuBF_4$ (+0.1 mM Br^-), electrolyte III, RE.

Table 2. Thickness and densities of PPy/WO_3 layers
d_n = nominal thickness, d = measured thickness after the jump method; ρ_{th} = density of the compact material, ρ_F = density, measured by the flotation method, ρ_J = density, calculated from d

Electrolyte	$d_n/\mu m$	c_C/wt %	$d/\mu m$	$\rho_{th}/g\,cm^{-3}$	$\rho_F/g\,cm^{-3}$	$\rho_J/g\,cm^{-3}$	P/%
I (MeCN)	3	0	4	1.50	1.50	1.1	25
	3	10	3.6	1.63	1.65	1.3	17
	3	30	5.0	1.97	1.96	1.2	40
II (H_2O)	3	0	3.4	1.55	1.55	1.35	12
	3	10	2.3	1.68	1.73	2.2 (?)	?
	3	30	3.1	2.02	2.06	1.95	3
III (H_2O)*	10	0	14	1.55	1.55	1.1	29
	10	10	13	1.68	1.73	1.3	23
	10	30	13.5	2.02	2.06	1.5	26

*See Fig.11.

can be seen. Only two very broad lines for PPy are observed, due to the amorphous nature of the polymer matrix.

Tensile strength of free standing PPy and PPy/WO_3-strips were measured. $\tau = 10$–$20\,N\,mm^{-2}$ was found for samples from the organic electrolyte I, which is close to the blank PPy, reported elsewhere [44–47]. This compared well with values for commodity plastic materials, e.g. PVC, PP, ABS or PTFE: $25\,N\,mm^{-2}$. Composites from aqueous electrolyte were brittle and could not be evaluated with reliability.

The electronic conductivities of the free standing foils were investigated using four probe techniques. According to Fig. 12(a), the specific conductivity of the blank PPy, made from electrolyte I (MeCN), is about $80\,S\,cm^{-1}$, well in the order reported in the literature [3, 4]. However, a strong decrease is observed in the presence of WO_3, which appreciably exceeds the effect expected by the admixture of an insulating filler according to

$$\kappa = \kappa_0 \frac{V_{PPy}}{V_{PPy} + V_{WO_3}} \qquad (11)$$

This finding may be due to the highly porous structure of the composite, as shown previously. In the case of PPy synthesized from the aqueous electrolyte II, the low specific conductivity of the matrix, about $1\,S\,cm^{-1}$, remains constant up to high WO_3 concentrations, *cf.* Fig. 12(b). Somewhat higher values, $8\,S\,cm^{-1}$, were reported previously [1]. It is at the highest WO_3 loadings, that κ begins to rise. A possible explanation may be the induction of a higher crystallinity in the PPy matrix, induced by the presence of the WO_3 crystals.

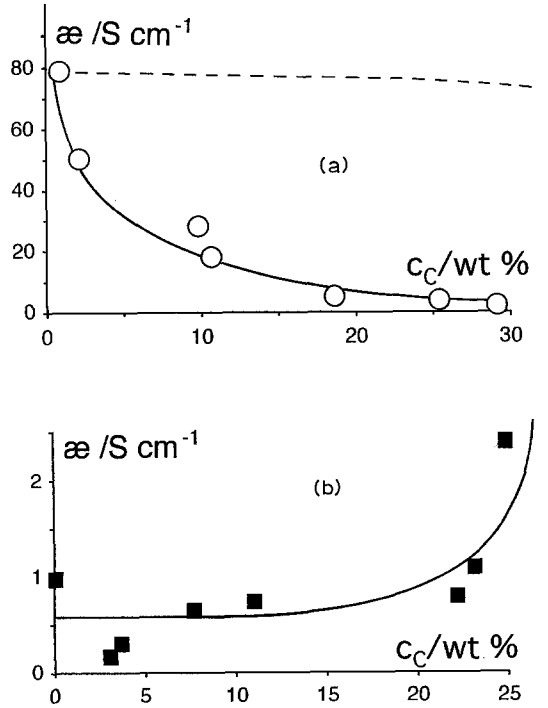

Fig. 12. Specific electronic conductivities of PPy/WO_3-composites in dependency on the concentration of WO_3 in the solid, $d_n = 10\mu m$. (a) From electrolyte I (MeCN), (·····) theoretical line, and (b) from electrolyte II (H_2O).

Acknowledgements

Financial support of this work by Deutsche Forschungsgemeinschaft (DFG) is gratefully acknowledged. We are indebted to Dr Krohn of this laboratory for technical assistance in the course of the photoelectrochemical measurements and to Mr Ibsch, Inorganic Chemistry, University of Duisburg, for kindly performing the X-ray diffraction measurements.

References

[1] A. Dall'Olio, Y. Dascota, V. Varacca and V. Bocchi, *C.R. Acad. Sci., Ser. C.* **267** (1968) 433.
[2] L. F. Warren and D. P. Anderson, *J. Electrochem. Soc.* **134** (1987) 101.
[3] A. F. Diaz, K. K. Kanizawa and G. P. Gardini, *J. Chem. Soc. Chem. Commun.* **854** (1979).
[4] A. F. Diaz, *Chem. Scripta* **17** (1981) 145.
[5] H. Naarmann, *Makromol. Chem., Macromol Symp.* **8** (1987) 1.
[6] B. Wessling, *Synthetic Metals* **27** (1988) A 83; *ibid.* **41** (1991) 1057.
[7] H. Yoneyama, Y. Shoji and K. Kawai, *Chem. Lett.* (1989) 1067.
[8] K. Kawai, N. Mihara, S. Kuwabata and H. Yoneyama, *J. Electrochem. Soc.* **137** (1990) 1793.

[9] O. Ikeda and H. Yoneyama, *J. Electroanal. Chem.* **265** (1989) 323.
[10] N. Furukawa, T. Saito and C. Iwakura, *Chemistry Express* **5** (1990) 269.
[11] F. Beck, M. Dahlhaus and N. Zahedi, *Electrochim. Acta* **37** (1992) 1265.
[12] F. Beck and M. Dahlhaus, *J. Appl. Electrochem.*, accepted.
[13] P. W. Martin, *Metal Finish. J.* (10) (1965) 399.
[14] I. Rajagopal, *in* 'Surface Modification Technologies', (edited by T. S. Sudarshan), Marcel Dekker, New York (1989) pp. 1–47.
[15] F. Beck and R. Michaelis, *J. Coat. Techn.* **64** (May 1992) 59.
[16] A. F. Diaz and J. I. Castillo, *J. Chem. Soc., Chem. Commun.* (1980) 397.
[17] F. Beck, J. Jiang, M. Kolberg, H. Krohn and F. Schloten, *Z. physik. Chem. n.f.* **160** (1988) 83.
[18] M. Amjad, D. Pletcher and C. Smith, *J. Electrochem. Soc.* **124** (1977) 203.
[19] I. F. Chang, B. L. Gilbert and T. I. Sun, *J. Electrochem. Soc.* **122** (1975) 955.
[20] M. Ladouleur, J. P. Dodelet, G. Tourillon, L. Parent and S. Dallaire, *J. Phys. Chem.* **94** (1990) 4579.
[21] V. V. Krasko, A. A. Yakovleva and Ya. M. Kolotyrkin, *Elektrokhimiya* **22** (1986) 1432.
[22] F. Beck, P. Braun and M. Oberst, *Ber. Bunsenges. Phys. Chem.* **91** (1987) 967.
[23] J. B. Schlenoff, Y. Fong and H. Xu, *Polym. Mater. Sci. Engng.* **63** (1990) 411.
[24] T. Inoue and. T. Yamase, *Bull. Chem. Soc. Jap.* **56** (1983) 985.
[25] J. A. de Saja and K. Tanaka, *Phys. Stat. Sol.* **108** (1988) K109.
[26] M. Kalaji, L. Nyholm, L. M. Peter and A. J. Rudge, *J. Electroanal. Chem.* **310** (1991) 113.
[27] J. Desilvestro and O. Haas, *Electrochim. Acta* **36** (1991) 361.
[28] D. Yaohua and M. Shaolin, *ibid.* **36** (1991) 2015.
[29] R. Kessel and J. W. Schultze, *Surf. & Interf. Anal.* **16** (1990) 401.
[30] H. Gerischer, *J. Electroanal. Chem.* **58** (1975) 263.
[31] G. Hodes, D. Cahen and J. Manassen, *Nature* **60** (1976) 312.
[32] W. Gissler and R. Memming, *J. Electrochem. Soc.* **124** (1977) 1711.
[33] B. Reichman and A. J. Bard, *ibid.* **126** (1979) 2133.
[34] S. Bhattacharyya, A. Roy and S. Aditya, *J. Indian Chem. Soc.* **66** (1989) 610.
[35] B. Reichman and A. J. Bard, *J. Electrochem. Soc.* **126** (1979) 583.
[36] F. Di Quarto, A. Di Paola and C. Sunseri, *Electrochim. Acta* **26** (1981) 1177.
[37] F. Di Quarto, A. Di Paola, S. Piazza and C. Sunseri, *Solar Energy Materials* **11** (1985) 419.
[38] A. M. Mance, M. A. Habib, S. P. Maheswari and S. J. Simko, *J. Appl. Electrochem.* **22** (1992) 501.
[39] H. H. Kung, H. S. Jarrett, A. W. Sleight and A. Ferreti, *J. Appl. Phys.* **48** (1977) 2463.
[40] R. S. Davidson and C. J. Willsher, *J. Appl. Electrochem.* **12** (1982) 517.
[41] F. Beck and M. Oberst, *Makromol. Chem., Macromol. Symp.* **8** (1987) 97.
[42] K. K. Kanazawa, A. F. Diaz, R. H. Geiss, W. D. Gill, J. K. Kwak, J. A. Logan, J. F. Rabolt and G. B. Street, *J. Chem. Soc., Chem. Commun.* (1979) 854.
[43] F. Beck, M. Oberst and P. Braun, *DECHEMA-Monogr.* **109** (1987) 457.
[44] D. Bloor, R. D. Hercliffe, C. G. Galiotis and R. J. Young, *in* Electronic Properties of Polymers and Related Compounds, (edited by H. Kuzmany *et al.*), Springer, Berlin (1985) p. 179.
[45] L. J. Buckley, D. K. Roylance and G. E. Wnek, *J. Polymer Aci., Part B: Polymer Phys.* **25** (1987) 2179.
[46] B. Sun, J. Jones, R. P. Burford and M. Skyllas-Kazacos, *J. Mater. Sci.* **24** (1989) 4024.
[47] R. C. D. Peres, J. M. Pernault and M.-A. de Paoli, *J. Polymer Sci., Part A: Polymer Chem.* **29** (2), (1991) 225.